

Joint Track Machine Learning

Andrew Jensen

March 9, 2023

Outline

Introduction

Motivation

Background

Historical Methods

Aims

Aim 1 - Joint Track Machine Learning

Aim 2 - Overcoming Single-Plane Limitations

Aim 3 - Pilot Human Study

Aim 4 - Standardized Kinematics Exam

Aim 5 - Joint Track Auto Toolkit

References

Introduction

Acknowledgments

I would like to thank the McJunkin Family Charitable Foundation for their generous grant that supports this work.

Motivation

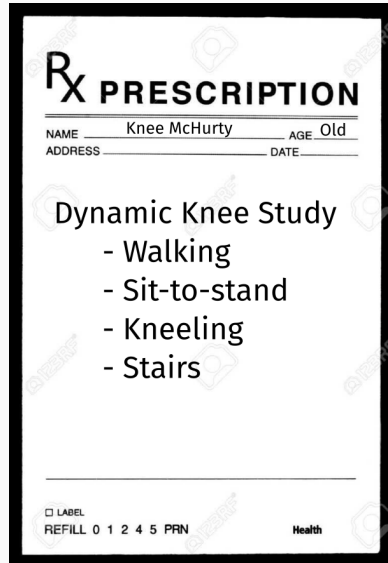
The Problem

- By 2030, roughly 3.5 million Total Knee Arthroplasty (TKA) will be performed in the US [15].
- 20% of patients receiving TKA are dissatisfied.
 - Instability, pain, unnatural [3, 5, 21].
- No reliable method of clinically assessing and quantifying joint dynamics.
 - Too much human supervision, too time consuming



Our Proposition

Orthopaedic surgeons and clinicians would readily adopt a practical and inexpensive technology that allows them to measure a patient's knee kinematics during activities of daily living.



Constraints

- It must fit within a standard clinical workflow
- The technology must utilize equipment commonly found in hospitals
- There must not be significant human supervision nor interaction to generate an examination report.



Background

Rigid Body Transformations

Translation

$$\begin{pmatrix} v'_x \\ v'_y \end{pmatrix} = \begin{pmatrix} v_x \\ v_y \end{pmatrix} + \begin{pmatrix} t_x \\ t_y \end{pmatrix}$$

→

$$\begin{pmatrix} v'_x \\ v'_y \\ 1 \end{pmatrix} = \begin{pmatrix} 1 & 0 & t_x \\ 0 & 1 & t_y \\ 0 & 0 & 1 \end{pmatrix} \begin{pmatrix} v_x \\ v_y \\ 1 \end{pmatrix}$$

Rigid Body Transformations

Rotations

$$R_x = \begin{pmatrix} 1 & 0 & 0 \\ 0 & c_x & -s_x \\ 0 & s_x & c_x \end{pmatrix}$$

$$R_y = \begin{pmatrix} s_y & 0 & c_y \\ 0 & 1 & 0 \\ c_y & 0 & -s_y \end{pmatrix}$$

$$R_z = \begin{pmatrix} c_z & -s_z & 0 \\ s_z & c_z & 0 \\ 0 & 0 & 1 \end{pmatrix}$$

Rigid Body Transformations

Homogeneous Transformation Matrices

$$\begin{aligned}\tilde{\vec{v}}' &= \begin{pmatrix} R_{3 \times 3} & \vec{t}_{3 \times 1} \\ 0 & 0 & 0 & 1 \end{pmatrix} \tilde{\vec{v}} \\ &= T_B^A \tilde{\vec{v}}\end{aligned}$$

Now we have a notation that allows us to describe arbitrary movement between reference frames.

Projective Geometry

$$\begin{pmatrix} x_s \\ y_s \\ z_s \\ 1 \end{pmatrix}_i = T_{\text{scene}}^{\text{cam}} \tilde{p}_i^{\text{obj}}$$

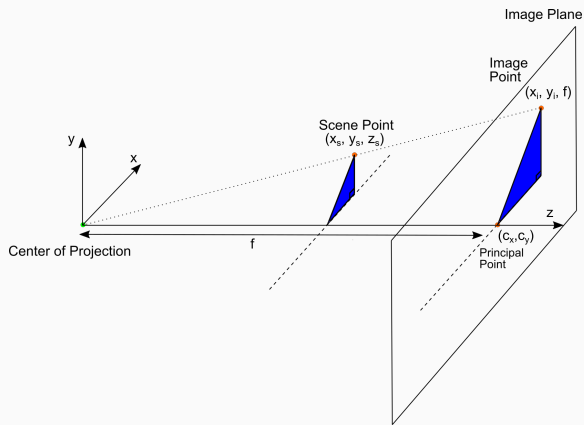
$$\begin{pmatrix} \tilde{x}_{\text{img}} \\ \tilde{y}_{\text{img}} \\ \tilde{z} \end{pmatrix} = \begin{pmatrix} f & 0 & 0 \\ 0 & f & 0 \\ 0 & 0 & 1 \end{pmatrix} \vec{x}_s$$

Where

$$x_{\text{img}} = \frac{\tilde{x}_{\text{img}}}{\tilde{z}} = \frac{f}{z_s} x_s$$

$$y_{\text{img}} = \frac{\tilde{y}_{\text{img}}}{\tilde{z}} = \frac{f}{z_s} y_s$$

Note: We are still in the camera's reference frame



Pixel Coordinates

Convert camera coordinates into image coordinates.

$$p_x = k_x x_{img} + c_x$$

$$p_y = k_y y_{img} + c_y$$

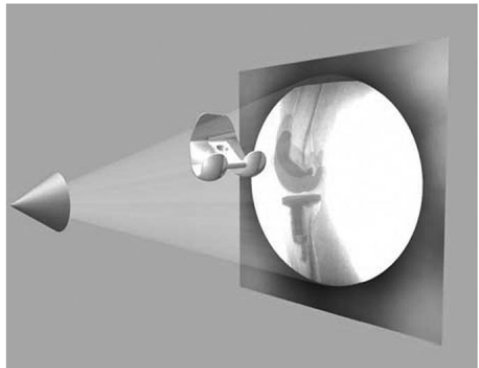
Where

$k \equiv$ Pixel Spacing

$c \equiv$ Image Focal Point

Model-Image Registration

If we know the projective parameters of the fluoroscopy machine, can we tinker with $T_{implant}^{cam}$ so that our virtual projection matches the fluoroscopic image?



From [19]

Historical Methods

Overview

Many different approaches have attempted to solve the model-image registration problem.

- Pre-computed projections
- Skin-mounted motion Capture
- Biplane Imaging
- Iterative Projections
- Model-based Roentgen Stereophotogrammetry

Pre-Computed Projections

- Saving space and memory by pre-computing as much as possible.
- Pre-computed distance maps [26, 17].
- Pre-computed shape libraries [4]

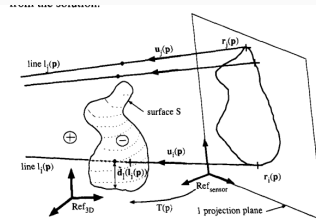
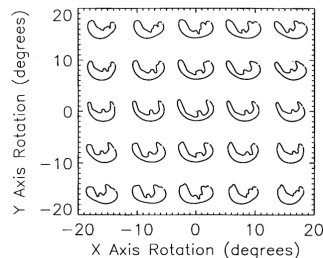


Fig. 2. Projection line to surface distance computation.

From [17]

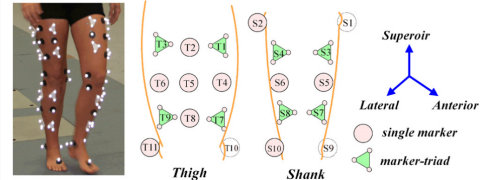


From [4]

Limitations of Pre-Computed Projections

- Requires an accurate contour from the input image in order to perform calculations.
 - Human supervision vs. inaccuracy.

Motion Capture (MoCap)



From [10]

- Can measure motion of MoCap beads very accurately.
- Skin-mounted [10, 14, 18].
- Bone pins [16] (any volunteers?).



From [16]

Limitations of Motion Capture

Skin Mounted

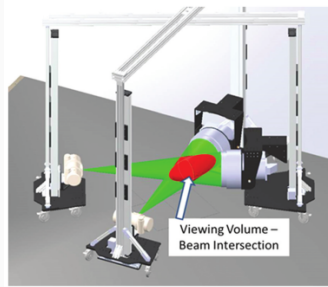
- Doesn't accurately describe underlying skeletal motion with clinical accuracy [10, 14, 18].

Bone Pins

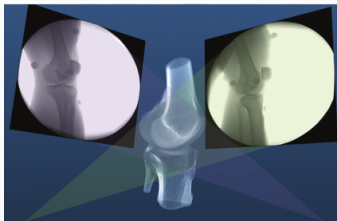
- Bone Pins
- Need I say more?

Biplane Imaging

- Utilizes multiple cameras to resolve 3D position and orientation[11, 7].
 - Highly accurate.
 - Gold Standard.



Both from [11]

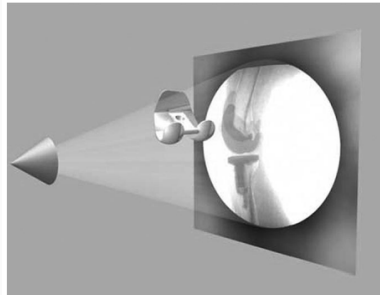


Limitations of Biplane Imaging

- Not many hospitals have biplane fluoroscopy setups.
- Clinically impractical

Iterative Projections

- Take advantage of modern computational graphics pipelines to quickly perform projection matching.
 - Image/Intensity similarity metrics [19]
 - Feature/Contour similarity metrics [9]



From [19]



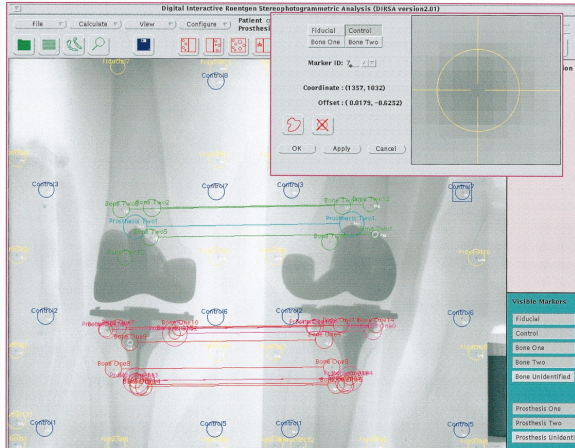
From [9]

Limitations of (historic) Iterative Projection Methods

- Requires human supervision for:
 - Pose initialization
 - Escaping local minima
 - Implant detection
- Chaotic and Noisy objective function

Model-based Roentgen Stereophotogrammetry (MBRSA)

- Uses implanted tantalum beads for motion tracking [24, 22]
- Extremely accurate [13, 20]
- Gold standard Measurement [6]



From [24]

Limitations of MBRSA

- Involves additional surgical procedures for inserting tantalum beads
- Human supervision
- Typically requires bi-plane imaging.

Aims

Aims

Aims 1/2

Joint Track Machine

Learning and Overcoming

Single-Plane Limitations

Aim 3/4

Pilot Trials and

Standardized Kinematics

Exam

Aim 5

Joint Track Auto Toolkit

Introduction

Motivation

Background

Historical Methods

Aims

Aim 1 - Joint Track Machine Learning

Aim 2 - Overcoming Single-Plane Limitations

Aim 3 - Pilot Human Study

Aim 4 - Standardized Kinematics Exam

Aim 5 - Joint Track Auto Toolkit

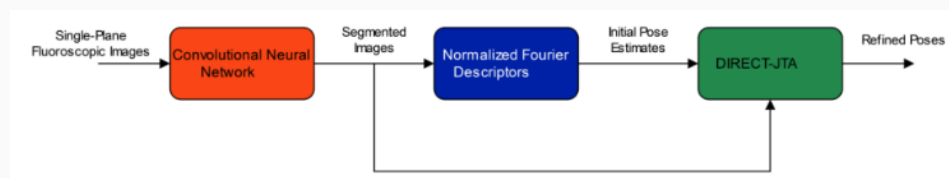
References

Goal

Demonstrate the feasibility of a fully autonomous, model-image registration pipeline.

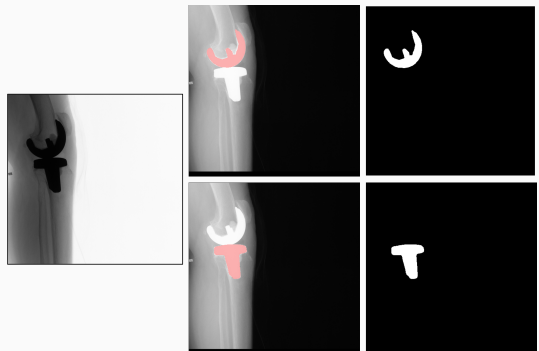
Method

- Three-tiered approach
 - Convolutional Neural networks (CNN) for autonomous implant detection
 - Normalized Fourier Descriptor shape libraries
 - Robust contour-based global optimization scheme



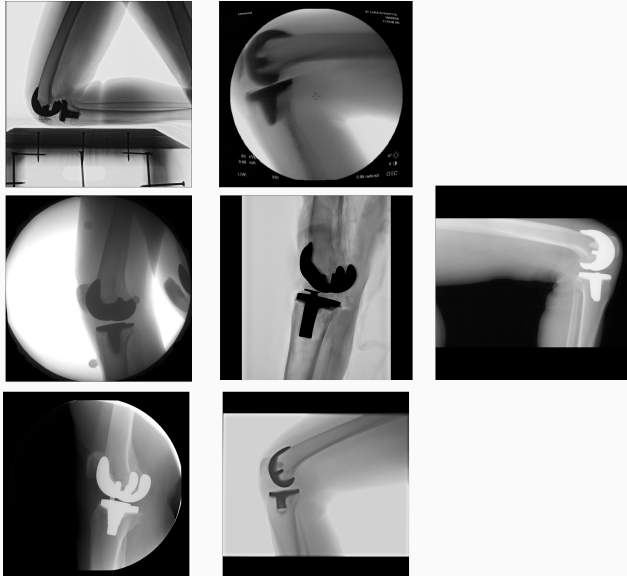
Autonomous Implant Detection Using Convolutional Neural Networks

- 2 CNNs
 - Femoral and Tibial implants
- High Resolution Network [25]



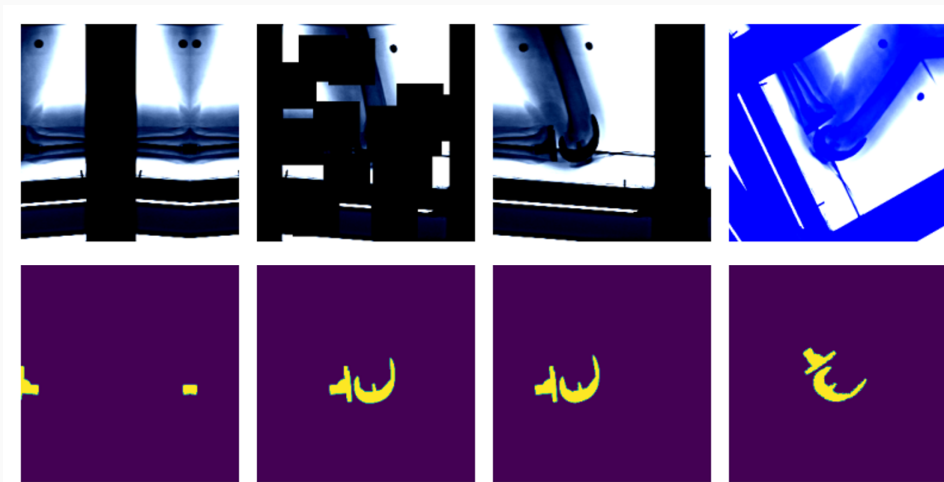
Neural Network Data

- ~8000 images
 - 7 TKA kinematics studies
 - PUT DATA INFO HERE!!!!



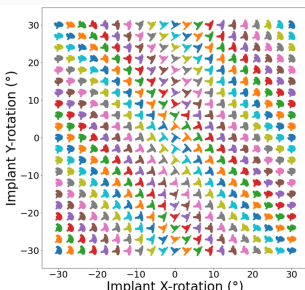
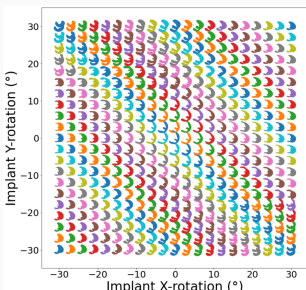
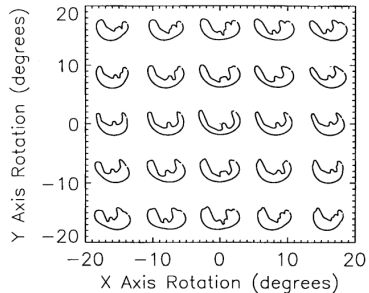
Neural Network Robustness

- Additional augmentations introduced during training [8].



Normalized Fourier Descriptor Shape Libraries

- Pose initialization using segmentation output.
- $\pm 30^\circ$ library span at 3° increments.



Pose Refinement Using Global Optimization

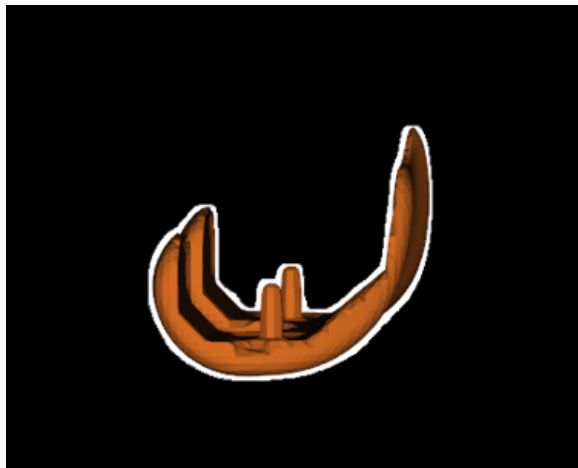
- Two main features
 - Objective function
 - Optimization routine

Contour-based Objective Function

- With accurate projection, contours provide a strong heuristic for orientation.
- Overlapping pixels between CNN segmentation and projected implant.
 - L_1 norm has quick parallel computation.

$$J = \sum_{i \in H} \sum_{j \in W} |I_{ij} - P_{ij}| = L_1(I, P)$$

- Sensitive to minor perturbations



Improving Robustness

- Dilation decreases sensitivity to perturbations.
- Multi-stage optimization can reduce dilation back to original edges.

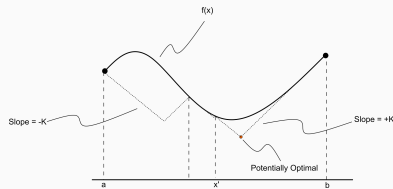
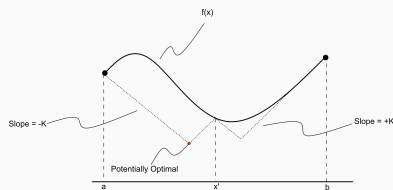
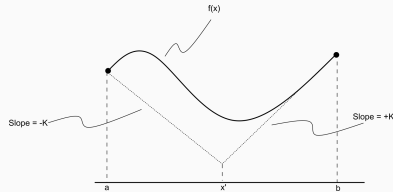


Optimization Routine

- No analytic form of the objective function exists, it **must** be sampled at points of interest.
 - Black Box Optimization [1, 2]

Lipschitzian Optimization

- Robust, global, black-box optimization routine if Lipschitz constant (K) is known [23].
- Lipschitz constant bounds the rate of change of a function.
- What if you don't know the Lipschitz constant?

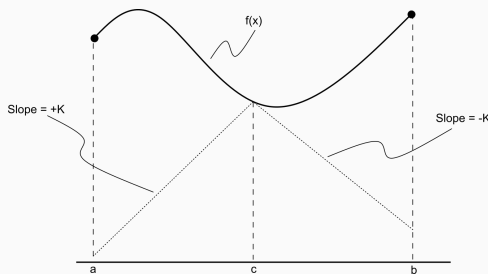


Lipschitzian Optimization without the Lipschitz Constant

Lipschitzian Optimization Without the Lipschitz Constant

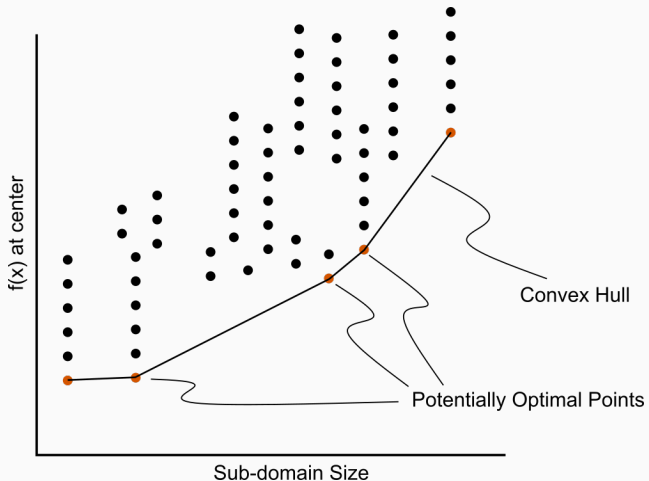
D. R. JONES,¹ C. D. PERTTUNEN,² AND B. E. STUCKMAN³

- Sample end-points instead of intersecting lines.
- Potentially optimal regions based on value at center and total size.
 - Trisect potentially optimal regions and re-sample centers



Determining Potentially Optimal Regions

- Convex hull of region size vs. center value



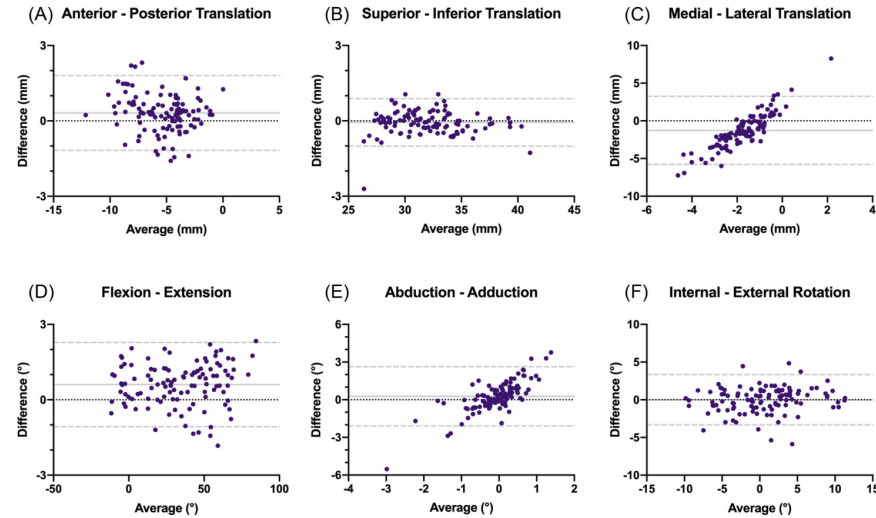
DiRECT for Joint Track Machine Learning

- Search region is along all 6 degrees of freedom.
 - Normalize to [0, 1].
- Three stages, each with decreasing levels of dilation.
 - Iteration budget for each stage.

Stage	Budget [Iterations]	Search Range [mm,deg]	Dilation (pixels)
“Tree”	~20,000	±45	5
“Branch”	~20,000	±25	3
“Leaf”	~10,000	±100 (z_{trans}) / ±3 (<i>else</i>)	1

Validation

- Achieved clinically acceptable accuracy [6, 12].



Awards

The work presented in this aim won the HAP Paul Award for Best Paper from the International Society for Technology in Arthroplasty's 2022 Annual Meeting.

Introduction

Motivation

Background

Historical Methods

Aims

Aim 1 - Joint Track Machine Learning

Aim 2 - Overcoming Single-Plane Limitations

Aim 3 - Pilot Human Study

Aim 4 - Standardized Kinematics Exam

Aim 5 - Joint Track Auto Toolkit

References

Goal

- The goal of this aim is to validation and test methods that can overcome single-plane limitations for model-image registration.
 - Out-of-plane (OOP) Translation
 - Symmetry Traps

Translation

- Depth perception is lost when using a single camera.
- Utilize a virtual “spring” to constrain relative OOP translation between implant components.

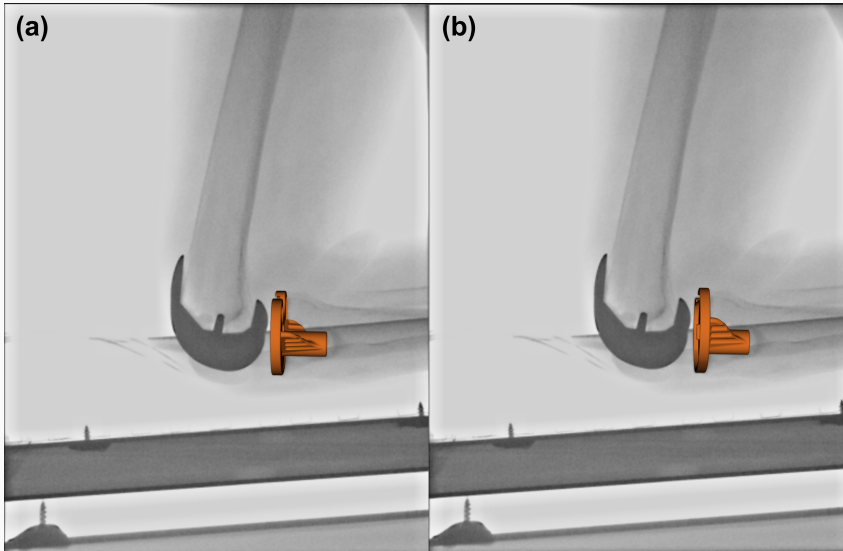
$$J = \alpha L_1(I, P) + \beta ML(Fem, Tib)$$

Where

$ML \equiv$ Relative mediolateral translation

Symmetry Traps

With a symmetric tibial implant, the contour is not always a perfect heuristic for true pose. Human operators typically utilize relative varus-valgus to determine correct pose.



Solving the Symmetric Pose

1. Create a vector from the camera origin to the implant origin (viewing ray).
2. Determine the axis (\vec{m}) and angle (θ) of rotation between the viewing ray and the symmetric (mediolateral) axis.
3. Rotate the implant -2θ about the same axis.
4. The final location is the symmetric pose of the object.

Five Approaches

- Virtual ligaments
- Binary selection between two poses
- Bland-Altman Calibration Constant
- Random Forest
- Fully Connected Network

Virtual Ligaments

$$J = \alpha L_1(I, P) + \beta ML(Fem, Tib) + \gamma VV(Fem, Tib)$$

Where

$VV \equiv$ Relative Varus-Valgus rotation

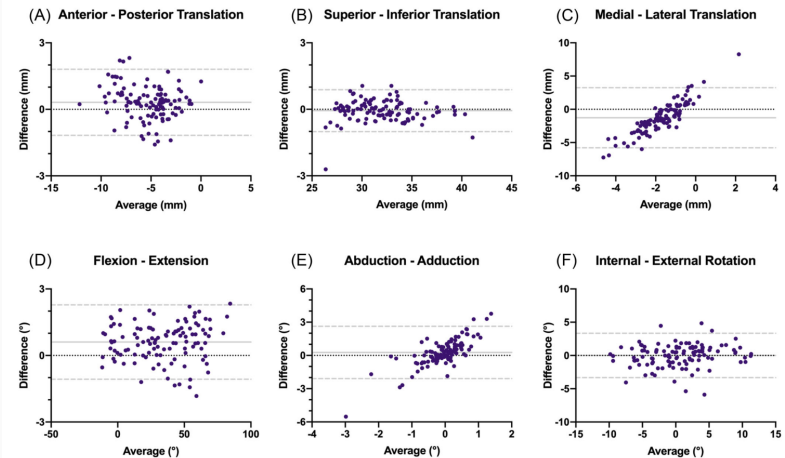
Binary Selection

1. Determine optimized pose using $L_1 + ML$
2. Calculate symmetric pose.
3. Pick pose with lower relative VV

This method can simplify the selection criteria (one fewer hyperparameter).

Bland-Altman Calibration Constant

- Utilizing Bland-Altmann plots from gold-standard kinematics, create a “correction constant” for relative varus/valgus angles.
- Notice linear trend in BA plots.



Introduction

Motivation

Background

Historical Methods

Aims

Aim 1 - Joint Track Machine Learning

Aim 2 - Overcoming Single-Plane Limitations

Aim 3 - Pilot Human Study

Aim 4 - Standardized Kinematics Exam

Aim 5 - Joint Track Auto Toolkit

References

Introduction

Motivation

Background

Historical Methods

Aims

Aim 1 - Joint Track Machine Learning

Aim 2 - Overcoming Single-Plane Limitations

Aim 3 - Pilot Human Study

Aim 4 - Standardized Kinematics Exam

Aim 5 - Joint Track Auto Toolkit

References

Introduction

Motivation

Background

Historical Methods

Aims

Aim 1 - Joint Track Machine Learning

Aim 2 - Overcoming Single-Plane Limitations

Aim 3 - Pilot Human Study

Aim 4 - Standardized Kinematics Exam

Aim 5 - Joint Track Auto Toolkit

References

References

References

- [1] Charles Audet and Warren Hare. *Derivative-Free and Blackbox Optimization*. Springer Series in Operations Research and Financial Engineering. Cham: Springer International Publishing, 2017. ISBN: 978-3-319-68912-8
978-3-319-68913-5. DOI: 10.1007/978-3-319-68913-5.
- [2] Ishan Bajaj, Akhil Arora, and M. M. Faruque Hasan. “Black-Box Optimization: Methods and Applications”. In: (Jan. 2021), pp. 35–65. DOI: 10.1007/978-3-030-66515-9_2.
- [3] P. N. Baker et al. “The Role of Pain and Function in Determining Patient Satisfaction After Total Knee Replacement: Data From the National Joint Registry for England and Wales”. In: *The Journal of Bone and Joint Surgery. British volume* 89-B.7 (July 2007), pp. 893–900. ISSN: 0301-620X, 2044-5377. DOI: 10.1302/0301-620X.89B7.19091.

References ii

- [4] S.A. Banks and W.A. Hodge. “Accurate Measurement of Three-Dimensional Knee Replacement Kinematics Using Single-Plane Fluoroscopy”. In: *IEEE Transactions on Biomedical Engineering* 43.6 (June 1996), pp. 638–649. ISSN: 00189294. DOI: 10.1109/10.495283.
- [5] Robert B. Bourne et al. “Patient Satisfaction after Total Knee Arthroplasty: Who Is Satisfied and Who Is Not?” In: *Clinical Orthopaedics & Related Research* 468.1 (Jan. 2010), pp. 57–63. ISSN: 0009-921X. DOI: 10.1007/s11999-009-1119-9.
- [6] Jordan S. Broberg et al. “Validation of a Machine Learning Technique for Segmentation and Pose Estimation in Single Plane Fluoroscopy”. In: *Journal of Orthopaedic Research* (Feb. 2023), jor.25518. ISSN: 0736-0266, 1554-527X. DOI: 10.1002/jor.25518.
- [7] William Burton et al. “Automatic Tracking of Healthy Joint Kinematics from Stereo-Radiography Sequences.”. In: *Computers in Biology and Medicine* (2021). DOI: 10.1016/j.combiomed.2021.104945.
- [8] Alexander Buslaev et al. “Albumentations: Fast and Flexible Image Augmentations”. In: *Information* 11.2 (Feb. 2020), p. 125. ISSN: 2078-2489. DOI: 10.3390/info11020125.

- [9] P. D. L. Flood and Scott A. Banks. “**Automated Registration of 3-D Knee Implant Models to Fluoroscopic Images Using Lipschitzian Optimization**”. In: *IEEE Transactions on Medical Imaging* 37.1 (2018), pp. 326–335. DOI: 10.1109/tmi.2017.2773398.
- [10] Bo Gao and Naiquan (Nigel) Zheng. “**Investigation of Soft Tissue Movement during Level Walking: Translations and Rotations of Skin Markers**”. In: *Journal of Biomechanics* 41.15 (Nov. 2008), pp. 3189–3195. ISSN: 00219290. DOI: 10.1016/j.jbiomech.2008.08.028.
- [11] John C. Ivester et al. “**A Reconfigurable High-Speed Stereo-Radiography System for Sub-Millimeter Measurement of In Vivo Joint Kinematics**”. In: *Journal of Medical Devices* 9.4 (Dec. 2015), p. 041009. ISSN: 1932-6181, 1932-619X. DOI: 10.1115/1.4030778.
- [12] Andrew Jensen et al. “**Joint Track Machine Learning: An Autonomous Method for Measuring 6DOF TKA Kinematics from Single-Plane x-Ray Images**”. In: *arXiv:2205.00057 [q-bio]* (Apr. 2022). arXiv: 2205.00057 [q-bio].

- [13] B L Kaptein et al. “**Evaluation of Three Pose Estimation Algorithms for Model-Based Roentgen Stereophotogrammetric Analysis**”. In: *Proceedings of the Institution of Mechanical Engineers, Part H: Journal of Engineering in Medicine* 218.4 (Apr. 2004), pp. 231–238. ISSN: 0954-4119, 2041-3033. DOI: 10.1243/0954411041561036.
- [14] Mei-Ying Kuo et al. “**Influence of Soft Tissue Artifacts on the Calculated Kinematics and Kinetics of Total Knee Replacements during Sit-to-Stand**”. In: *Gait & Posture* 33.3 (Mar. 2011), pp. 379–384. ISSN: 09666362. DOI: 10.1016/j.gaitpost.2010.12.007.
- [15] Steven Kurtz et al. “**Projections of Primary and Revision Hip and Knee Arthroplasty in the United States from 2005 to 2030:**” in: *The Journal of Bone & Joint Surgery* 89.4 (Apr. 2007), pp. 780–785. ISSN: 0021-9355. DOI: 10.2106/JBJS.F.00222.
- [16] Mario A. Lafontaine et al. “**Three-Dimensional Kinematics of the Human Knee during Walking.**”. In: *Journal of Biomechanics* (1992). DOI: 10.1016/0021-9290(92)90254-x.

- [17] S. Lavallee and R. Szeliski. “**Recovering the Position and Orientation of Free-Form Objects from Image Contours Using 3D Distance Maps**”. In: *IEEE Transactions on Pattern Analysis and Machine Intelligence* 17.4 (Apr. 1995), pp. 378–390. ISSN: 01628828. DOI: 10.1109/34.385980.
- [18] Cheng-Chung Lin et al. “**Effects of Soft Tissue Artifacts on Differentiating Kinematic Differences between Natural and Replaced Knee Joints during Functional Activity**”. In: *Gait & Posture* 46 (May 2016), pp. 154–160. ISSN: 09666362. DOI: 10.1016/j.gaitpost.2016.03.006.
- [19] M.R. Mahfouz et al. “**A Robust Method for Registration of Three-Dimensional Knee Implant Models to Two-Dimensional Fluoroscopy Images**”. In: *IEEE Transactions on Medical Imaging* 22.12 (Dec. 2003), pp. 1561–1574. ISSN: 0278-0062. DOI: 10.1109/TMI.2003.820027.
- [20] Tuuli Saari et al. “**Knee Kinematics in Medial Arthroscopy. Dynamic Radiostereometry during Active Extension and Weight-Bearing**”. In: *Journal of Biomechanics* 38.2 (Feb. 2005), pp. 285–292. ISSN: 00219290. DOI: 10.1016/j.jbiomech.2004.02.009.

- [21] C. E. H. Scott et al. “Predicting Dissatisfaction Following Total Knee Replacement: A Prospective Study of 1217 Patients”. In: *The Journal of Bone and Joint Surgery. British volume* 92-B.9 (Sept. 2010), pp. 1253–1258. ISSN: 0301-620X, 2044-5377. DOI: 10.1302/0301-620X.92B9.24394.
- [22] Göran Selvik. “Roentgen Stereophotogrammetry: A Method for the Study of the Kinematics of the Skeletal System”. In: *Acta Orthopaedica Scandinavica* 60.sup232 (Jan. 1989), pp. 1–51. ISSN: 0001-6470. DOI: 10.3109/17453678909154184.
- [23] Bruno O. Shubert. “A Sequential Method Seeking the Global Maximum of a Function”. In: *SIAM Journal on Numerical Analysis* 9.3 (1972), pp. 379–388. DOI: 10.1137/0709036. eprint: <https://doi.org/10.1137/0709036>.
- [24] Henri A Vrooman et al. “Fast and Accurate Automated Measurements in Digitized Stereophotogrammetric Radiographs”. In: *Journal of Biomechanics* 31.5 (May 1998), pp. 491–498. ISSN: 00219290. DOI: 10.1016/S0021-9290(98)00025-6.
- [25] Jingdong Wang et al. “Deep High-Resolution Representation Learning for Visual Recognition”. In: *arXiv:1908.07919 [cs]* (Mar. 2020). arXiv: 1908.07919 [cs].

- [26] S. Zuffi et al. “A Model-Based Method for the Reconstruction of Total Knee Replacement Kinematics”. In: *IEEE Transactions on Medical Imaging* 18.10 (Oct./1999), pp. 981–991. ISSN: 02780062. DOI: 10.1109/42.811310.